Testing the multi-configuration time-dependent Hartree–Fock method

2004 J. Phys. B: At. Mol. Opt. Phys. 37 763

(http://iopscience.iop.org/0953-4075/37/4/004)

INSTITUTE OF PHYSICS PUBLISHING JOURNAL OF PHYSICS B: ATOMIC, MOLECULAR AND OPTICAL PHYSICS

J. Phys. B: At. Mol. Opt. Phys. **37** (2004) 763–773 PII: S0953-4075(04)66931-8

Testing the multi-configuration time-dependent Hartree–Fock method

Jürgen Zanghellini[1], **Markus Kitzler**[1], **Thomas Brabec**[1] **and Armin Scrinzi**[2]

[1] Center for Photonics Research, University of Ottawa, Ottawa, ON K1N 6N5, Canada
[2] Institut für Photonik, Technische Universität Wien, Gusshausstrasse 27, A-1040 Wien, Austria

E-mail: zanghellini@tuwien.ac.at and scrinzi@tuwien.ac.at

Received 28 July 2003, in final form 19 December 2003
Published 30 January 2004
Online at stacks.iop.org/JPhysB/37/763 (DOI: 10.1088/0953-4075/37/4/004)

Abstract

We test the multi-configuration time-dependent Hartree–Fock method as a new approach towards the numerical calculation of dynamical processes in multi-electron systems using the harmonic quantum dot and one-dimensional helium in strong laser pulses as models. We find rapid convergence for quantities such as ground-state population, correlation coefficient and single ionization towards the exact results. The method converges, where the time-dependent Hartree–Fock method fails qualitatively.

1. Introduction

The single active electron approximation is one of the cornerstones of the theory of intense laser–matter interaction [1–3]. It is based on the assumption that only the weakest bound electron of an atom or molecule interacts with the laser field. The other electrons remain inert. Although this has proved to be a good approximation for atoms, recent experiments [4, 5] have clearly demonstrated that for the description of more complex systems, such as molecules and clusters, the single active electron approximation fails.

On the theory side, the interaction of strong laser pulses with complex systems requires the handling of many-body processes and non-perturbative dynamics, which pose difficult theoretical and computational problems. Straightforward numerical solutions for systems containing more than two electrons [6–8] seem to be out of question. This has spawned great interest in the development of approximate, numerical methods that capture the essential physics and are still computationally feasible. The two main approaches investigated so far are the time-dependent density functional theory [9, 10] and the time-dependent Hartree–Fock (TDHF) method [11–16]. Both methods do not perform well in describing correlated multi-electron dynamics. Moreover, neither method allows convergence to the exact result, which makes it hard to determine the quality of a calculation.

0953-4075/04/040763+11$30.00

Multi-configuration methods, on the other hand, are known to accurately describe physical properties and are widely used in atomic structure calculations [17]. We have recently introduced a new approach called the multi-configuration time-dependent Hartree–Fock (MCTDHF) method [18]. In contrast to standard multi-configuration methods, in our approach the mean field of the electron density contains a time-dependent potential. Our implementation is based on the multi-configuration time-dependent Hartree method of [19], from which it differs in the anti-symmetrization of the electronic wavefunction and in the calculation of the electron–electron interaction. The MCTDHF method presents a generalization of the time-dependent Hartree–Fock method. Instead of using a single Slater determinant, in MCTDHF one expands the multi-electron wavefunction into several determinants, or 'configurations'. The MCTDHF wavefunction converges to the exact solution in the limit of an infinite number of configurations.

The aim of this paper is to assess the reliability and efficiency of the MCTDHF approach and to determine the number of configurations needed for convergence. This is done by considering two one-dimensional (1D) examples, namely the laser driven motion of two electrons in a harmonic oscillator potential and the electron dynamics of a helium atom irradiated by a short, intense laser pulse. In both cases we solve the time-dependent Schrödinger equation (TDSE) by using the MCTDHF ansatz and compare with their (numerically) exact counterparts. We investigate quantities such as the ground-state occupation, correlation coefficient, and single and double ionization, where we find convergence of MCTDHF towards the full TDSE results with a moderate number of configurations. For certain observables such as ground-state electron density or double ionization, where TDHF is known to fail, this represents not only a gradual, but also a qualitative improvement, while the computational efficiency of TDHF is retained.

2. Multi-configuration time-dependent Hartree–Fock theory

Our analysis starts from the TDSE (in atomic units),

$$\mathrm{i}\dot{\Psi}(x, y; t) = H(x, y; t)\Psi(x, y; t) \tag{1}$$

for a two-electron system with a fixed nucleus described by the Hamiltonian H.

In MCTDHF one approximates the exact wavefunction by the ansatz

$$\Psi(x, y; t) = \sum_{j_1=1}^{n}\sum_{j_2=1}^{n} A_{j_1 j_2}(t)\varphi_{j_1}(x; t)\varphi_{j_2}(y; t)\left|s_{j_1}\right\rangle \otimes \left|s_{j_2}\right\rangle \tag{2}$$

where both the linear expansion coefficients $A_{j_1 j_2}(t)$ and the single particle functions $\varphi_j(x; t)$ are time-dependent. Here $s_j = \pm 1/2$ is the spin part associated with expansion function φ_j. Ansatz (2) is not unique and therefore requires additional constraints [19], which were chosen as

$$\langle s_i|s_j\rangle\langle\varphi_i(x; t)|\varphi_j(x; t)\rangle = \delta_{ij} \tag{3a}$$

$$\langle s_i|s_j\rangle\langle\varphi_i(x; t)|\dot{\varphi}_j(x; t)\rangle = 0. \tag{3b}$$

Note that the ansatz is complete in the limit $n \to \infty$.

Until now we have made no reference to the antisymmetry of the electron wavefunction. As the Hamiltonian and therefore the propagation equations are fully symmetric under exchange of electrons, an initially antisymmetric wavefunction stays antisymmetric during propagation. It is therefore sufficient to demand that the initial coefficients A be fully antisymmetric with respect to their indices. In our case of only two electrons this means $A_{j_1 j_2} = -A_{j_2 j_1}$, which reduces the number of independent configurations to $n(n-1)/2$.

The time evolution equations for $A_{j_1 j_2}$ and φ_{j_i} are obtained from the Dirac–Frenkel variational principle [20, 21]

$$\langle \delta\Psi | i\,\partial_t - H|\Psi\rangle = 0. \tag{4}$$

Following [19] we define the single-hole function

$$\Psi^{(l)}(y;t) = \langle \varphi_l(x;t) \otimes s_l | \Psi(x,y;t)\rangle = \sum_{j_2=1}^{n} A_{l j_2}(t)\varphi_{j_2}(y;t)\big|s_{j_2}\big\rangle, \tag{5}$$

the mean field operator

$$\langle \mathbf{H}\rangle_{j,l} = \langle \Psi^{(j)} | H | \Psi^{(l)}\rangle, \tag{6}$$

the density matrix

$$\tilde{\boldsymbol{\rho}}_{j,l} = \langle \Psi^{(j)} | \Psi^{(l)}\rangle \tag{7}$$

as well as the projector on the space spanned by the single-particle functions

$$P = \sum_{j=1}^{n} |\varphi_j \otimes s_j\rangle\langle \varphi_j \otimes s_j|. \tag{8}$$

Performing the variation in (4) one obtains the nonlinear equations [19]

$$\mathrm{i}\dot{A}_{j_1 j_2} = \sum_{l_1,l_2}^{n} \big\langle s_{j_1}\big|s_{l_1}\big\rangle \big\langle s_{j_2}\big|s_{l_2}\big\rangle \big\langle \varphi_{j_1}\varphi_{j_2}\big|H\big|\varphi_{l_1}\varphi_{l_2}\big\rangle A_{l_1 l_2} \tag{9a}$$

$$\mathrm{i}\dot{\boldsymbol{\varphi}} = (1-P)\tilde{\boldsymbol{\rho}}^{-1}\langle \mathbf{H}\rangle \boldsymbol{\varphi} \tag{9b}$$

with $\boldsymbol{\varphi} = (\varphi_1 \otimes s_1, \ldots, \varphi_n \otimes s_n)^{\dagger}$ in vector notation.

In the limit of $n = 2$ one obtains the single-configuration (time-dependent) Hartree–Fock method [15]. For singlet spin the spatial part of our wavefunction takes the form $\varphi_1(x)\varphi_2(y) + \varphi_2(x)\varphi_1(y)$. Note that there are no constraints on the relation between φ_1 and φ_2, they neither need to be identical nor orthogonal—unlike most versions of the Hartree–Fock method, our implementation is 'unrestricted'.

In the same way as TDHF, MCTDHF with a finite number of configurations also suffers, in principle, from the problem of nonlinearity of the evolution equations [22] which may lead to a violation of the superposition principle. However, in the case of MCTDHF this problem is greatly reduced, which can be illustrated on the counter-example for TDHF used in [22]. MCTDHF, by construction (equation (2)), can describe the superposition of, say, a fractional occupation of the neutral ground state (one configuration) plus a state consisting of a polarized ionic core with one electron far removed (second configuration). This is a situation where TDHF manifestly fails. Analogously more complex superposition states may require additional configurations, but in the theoretical limit of infinitely many configurations the wavefunction converges towards the linear TDSE.

Our method is also quite distinct from other theories such as the state specific expansion approach (SSEA) [23]. While in the latter it is necessary to identify the major correlation effects and to adjust the approximated expansion accordingly, MCTDHF does not require any *a priori* knowledge, since for every time step and fixed number of configurations an optimal expansion is warranted by the variational principle.

We want to point out that besides the good convergency, which we demonstrate in the following, the true power of the method lies in its favourable scaling behaviour with the number of electrons. Whereas the number of points in straightforward discretization increases exponentially with the number of particles f, MCTDHF scales linearly $\propto n \geqslant f$ for the

factor functions φ and the number of coefficients A only increases like $\sim\binom{n}{f}$ due to their antisymmetry. Therefore it seems possible to study the correlated dynamics of few electron systems with up to ten electrons without making severe approximations.

The propagation equations were solved using a finite-difference representation of the factor functions $\varphi_j(x)$ on a one-dimensional grid. The time-integration is performed by a self-adaptive, high-order Runge–Kutta integrator.

3. The harmonic quantum dot

We first test our approach on the laser driven dynamics of two electrons in a harmonic oscillator potential, for which a semi-analytic solution is available for comparison. The Hamiltonian H in equation (1) for the harmonic quantum dot reads

$$H(x, y; t) = -\frac{1}{2}\left(\partial_x^2 + \partial_y^2\right) + \frac{\Omega^2}{2}(x^2 + y^2) + \frac{1}{\sqrt{(x-y)^2 + a^2}} + (x + y)\mathcal{E}_0 \sin(\omega t). \tag{10}$$

The interaction between the electrons is modelled by a 'smoothed Coulomb' potential [24] with shielding parameter a. The electrons are coupled to a monochromatic laser field with frequency ω and amplitude $\mathcal{E}_0$, which is described in dipole approximation and length gauge. Finally, Ω denotes the frequency of the harmonic oscillator.

Hamiltonian (10) separates when expressed in new coordinates

$$R = \tfrac{1}{2}(x + y) \qquad \text{and} \qquad r = x - y \tag{11}$$

which allows us to write the spatial part of the wavefunction in the factorized form

$$\Psi = \mathrm{e}^{-\mathrm{i}\epsilon t}\phi(r)\psi(R; t). \tag{12}$$

The factors $\phi(r)$ and $\psi(R; t)$ are determined by the equations

$$\epsilon\phi(r) = \left(-\partial_r^2 + \frac{\Omega^2 r^2}{4} + \frac{1}{\sqrt{r^2 + a^2}}\right)\phi(r). \tag{13}$$

and

$$\mathrm{i}\dot{\psi}(R; t) = \left(-\tfrac{1}{4}\partial_R^2 + \Omega^2 R^2 - 2R\mathcal{E}_0 \sin(\omega t)\right)\psi(R; t). \tag{14}$$

The lowest eigenvalue ϵ belongs to an $x \leftrightarrow y$ exchange symmetric, even function $\phi(r)$, i.e. the singlet ground state. While (13) can in general only be solved numerically, the solution of the harmonic oscillator problem (14) can be given in closed form [25] for an arbitrary initial state wavefunction $\psi(R; 0)$, which we have chosen as the field-free ground state.

To determine the correlation of a system we use a measure suggested in [26]. The idea of that measure is based on the existence of a uniquely defined representation of the wavefunction in terms of single-electron orbitals, for which the single-particle density matrix becomes 2×2 block-diagonal. In this canonical representation one writes the wavefunction as

$$\Psi(x, y; t) = \sum_i p_i(t)\Phi_i(x, y; t) \tag{15}$$

where Φ_i denotes a Slater determinant consisting of the two single-electron orbitals belonging to the same diagonal block and $|p_i|^2$ is its occupation probability. Correlation is identified with the number of different determinants Φ_i needed to approximate the exact wavefunction. Normalization of Ψ requires $\sum_i |p_i|^2 = 1$. A 'degree of correlation' K is defined as the following measure for the 'length' of the sum (15)

$$K(t) = \frac{1}{\sum_i |p_i(t)|^4}. \tag{16}$$

Table 1. Initial energy E_η and degree of correlation K_η for an increasing number of configurations η. $\eta = \infty$ refers to the exact values.

n	$\eta = \binom{n}{2}$	E_η	$\frac{E_\eta - E_\infty}{E_\infty}$	K_η	$\frac{K_\eta - K_\infty}{K_\infty}$
2	1	1.1795	0.4301	1.0000	−0.4100
4	6	1.0214	0.2384	1.3568	−0.1996
6	15	0.8261	0.0016	1.7260	0.0181
8	28	0.8255	0.0009	1.7150	0.0117
10	45	0.8250	0.0002	1.7029	0.0045
12	66	0.8249	0.0001	1.6998	0.0027
∞	∞	0.8247	0.0000	1.6951	0.0000

K does not depend on a specific representation of the wavefunction, except for choosing the single-electron coordinates (x, y). For practical purposes it is useful to note that K can be calculated without explicit reference to the canonical representation by using the single-particle density operator ρ, whose kernel is given by

$$\rho(x', x; t) = \int \Psi(x', y; t)\Psi^*(x, y; t)\,\mathrm{d}y. \tag{17}$$

The eigenvalues of ρ are the desired expansion coefficients $|p_i|^2$.

For our tests we have chosen $\Omega = 0.25$ (broad harmonic potentials) and $a = 0.25$, where correlation is high ($K = 1.695$). We used a lattice range of ± 10 with uniform grid spacing of 0.1. The execution time of the program on a 1.8 GHz PC for a typical calculation with 15 configurations was less than 1 h.

Table 1 lists the ground-state energy E_η of the system together with the degree of correlation K_η as a function of the number η of MCTDHF configurations. In contrast to real atomic and molecular systems, the ground-state energy of the harmonic oscillator is strongly modified by correlation. The correlation energy, i.e. the difference between single configuration Hartree–Fock and the exact energy is $E_1 - E_\infty = 0.3547$. For 15 configurations the overlap $|\langle\Psi_{15}|\Psi_\infty\rangle|^2$ between the MCTDHF and the exact ground-state wavefunction is 0.999 39. Convergence beyond that value is rather slow with an overlap of 0.999 89 for 66 configurations. It is interesting to note that K_η does not increase monotonically with η. This indicates that with fewer configurations the populations $|p_i|^2$ may be more evenly distributed for the variationally optimal energy E_η than for a large number of configurations.

The ground-state electron density distribution calculated by MCTDHF is plotted in figure 1 for various numbers of configurations. Good agreement is achieved for more than six configurations. Note that in the correct result the electrons tend to accumulate at two separate maxima, which differs qualitatively from the TDHF electron density with a single maximum at the centre.

Next we investigate the time evolution of our system. We find that correlation, K, varies only weakly during the evolution, not exceeding the level $\lesssim 10^{-5}$ even at field strength $\mathcal{E}_0 = 1$. The weak dynamical variation of correlation is not surprising, as in this system according to equation (13) electron–electron interaction can be fully separated from the interaction with the field. We use the overlap of the time-dependent wavefunction with the ground state $|\langle\Psi(x, y; 0)|\Psi(x, y; t)\rangle|^2$ to monitor the convergence of the dynamical behaviour of the system. Figure 2 shows the overlap for the parameters $\mathcal{E}_0 = 1$ and $\omega = 8\,\Omega$. In single configuration one sees significant deviations from the exact result. At times, the probability is overestimated and, more importantly, at other times it is reduced to almost 0. With six configurations the probability curve changes significantly giving a first estimate of the error

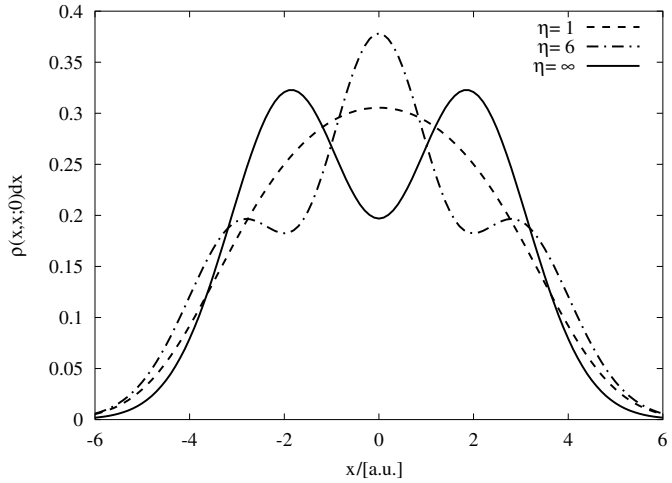

Figure 1. Electron density $\rho(x, x; 0)$ for the ground-state wavefunction and an increasing number of configurations η. ($\eta = \infty$ refers to the numerically exact solution.) The result for $\eta = 15$ coincides with the exact result within the resolution of the plot.

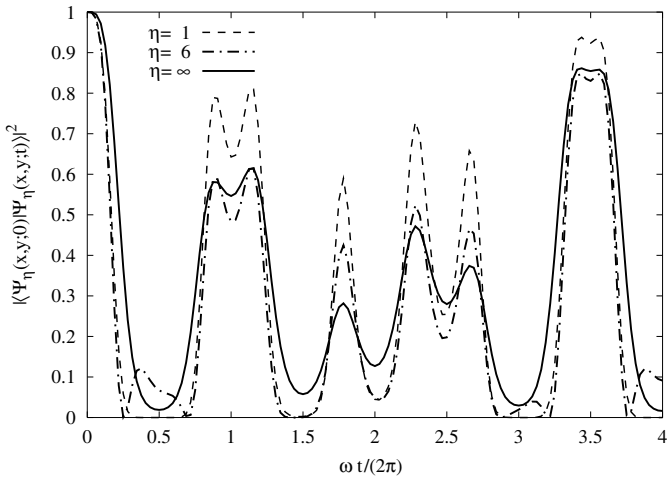

Figure 2. Probability of being in the ground state $|\langle\Psi_\eta(x, y; 0)|\Psi_\eta(x, y; t)\rangle|^2$ for an increasing number of configurations η ($\eta = \infty$ refers to the numerically exact solution) in the presence of an electric field of strength $\mathcal{E}_0 = 1$ and frequency $\omega = 8\,\Omega$. The result for $\eta = 15$ coincides with the exact result within the resolution of the plot.

of the single-configuration Hartree–Fock. The curve with 15 configurations already coincides with the exact calculation within a maximal absolute error of 0.004 582, which may be considered satisfactory accuracy.

4. The 1D helium atom

The helium atom is known to be one of the most strongly correlated atomic systems and serves as the basic testing ground for multi-electron calculations. Here we use a one-dimensional

Table 2. Ground-state energy $E_{0,\eta}$ and degree of correlation $K_\eta(0)$ for an increasing number of configurations η for the 1D helium atom. $\eta = \infty$ refers to the numerically exact values.

n	$\eta = \binom{n}{2}$	$E_{0,\eta}$	$\frac{E_{0,\eta}-E_{0,\infty}}{E_{0,\infty}}$	$K_\eta(0)$	$\frac{K_\eta(0)-K_\infty(0)}{K_\infty(0)}$
2	1	−2.8830	-6.62×10^{-3}	1.000 00	-1.66×10^{-2}
4	6	−2.8993	-9.91×10^{-4}	1.015 98	-8.98×10^{-4}
6	15	−2.9019	-1.07×10^{-4}	1.016 84	-5.38×10^{-5}
8	28	−2.9022	-3.10×10^{-5}	1.016 90	7.92×10^{-6}
10	45	−2.9022	-6.17×10^{-6}	1.016 90	6.00×10^{-6}
12	66	−2.9022	-2.17×10^{-6}	1.016 90	3.23×10^{-6}
∞	∞	−2.9022	0.00	1.016 90	0.00

helium model to investigate the performance of MCTDHF in describing single and double ionization.

The total time-dependent Hamiltonian H in equation (1) for our 1D helium atom irradiated by a laser field $\mathcal{E}(t)$ reads

$$H(x, y; t) = -\frac{1}{2}\left(\partial_x^2 + \partial_y^2\right) - \frac{2}{\sqrt{x^2 + b^2}} - \frac{2}{\sqrt{y^2 + b^2}} + \frac{1}{\sqrt{(x - y)^2 + b^2}} + (x + y)\mathcal{E}(t) \qquad (18)$$

where the electron–electron interaction and the electron–nucleus interaction are modelled by the usual 'smoothed Coulomb' potential with shielding parameter b. We set $b = 0.7408$ and solved the TDSE numerically on the full (1 + 1)-dimensional grid and by MCTDHF on the corresponding one-dimensional grid. The lattice range is chosen to ± 200 with a uniform grid spacing of 0.2. Propagating the field-free Hamiltonian in imaginary time results in a singlet ground-state energy of $E_0 = -2.9022$, which approximates the 3D ground-state energy of 3D helium.

Table 2 lists the ground-state energy $E_{0,\eta}$ of our helium model together with the degree of correlation $K_\eta(0)$ as a function of the number η of MCTDHF configurations. Both values vary only little with the number of configurations. As in the case of the harmonic quantum dot, they converge towards the exact values with increasing number of configurations. While correlation has a relatively little effect on the total energy, it strongly modifies the wavefunction at larger distances, where it produces noticeable pinches in the probability density along the diagonal $x = y$. This is shown in figure 3, where logarithmic contour maps of the ground-state probability density for various number of configurations are plotted. It is well known that a single configuration calculation does not reproduce those bumps, but with increasing configurations the structures are recovered. This can be quantified by the overlap: with $\eta = 15$ configurations $|\langle\Psi_{15}(x, y; 0|\Psi_\infty(x, y; 0)\rangle|^2 = 0.999\,94$, where Ψ_∞ denotes the numerically exact solution. For $\eta = 45$ the agreement is excellent, overlapping the exact wavefunction to 99.999%.

In order to analyse the dynamic quality of our approach the helium model is irradiated by a short, intense, linearly polarized laser pulse with frequency $\omega = 0.1837$ au (wavelength $\lambda = 248$ nm) and peak amplitude $\mathcal{E}_0 = 0.1894$ au (peak intensity $I = 1.26 \times 10^{15}$ W cm^{-2}). Thus the laser field has the form

$$\mathcal{E}(t) = \mathcal{E}_0 f(t) \sin(\omega t) \qquad (19)$$

where the envelope $f(t)$ is chosen to be trapezoidal, with 2-cycle turn-on and turn-off and a 2-cycle flat top.

To investigate the dynamic properties we show logarithmic contour maps of the probability density at the end of the laser pulse for various configurations (figure 4). All sub-figures are

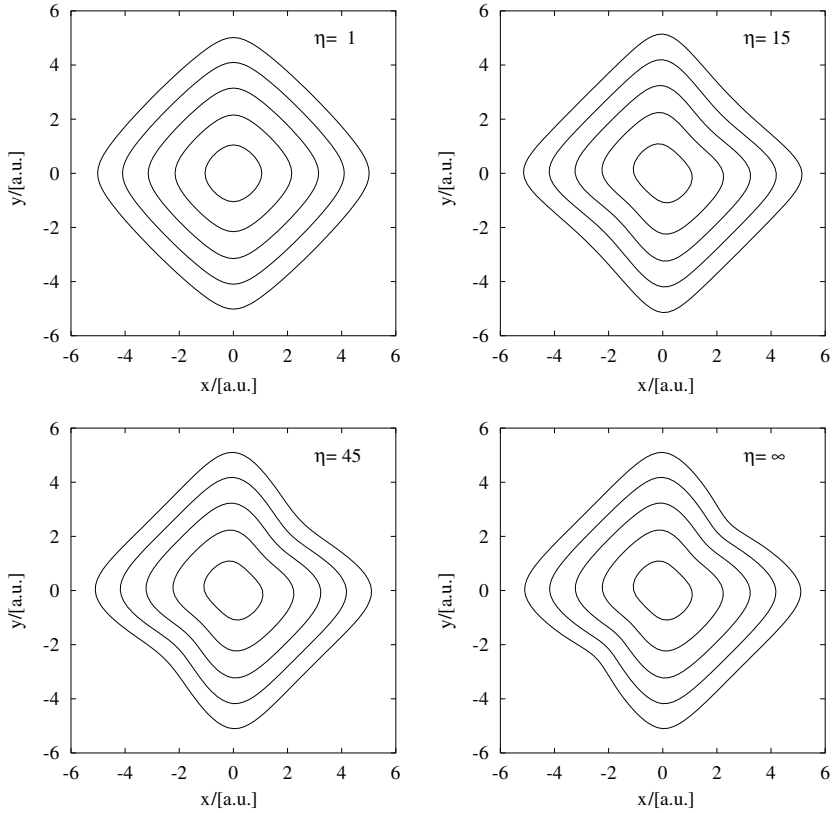

Figure 3. Logarithmic contour maps of the ground-state probability density of helium for various configurations η. ($\eta = \infty$ refers to the numerically exact solution.) Contours differ by a factor of 10, representing 0.1 for the innermost line.

dominated by probability flows along the x- and y-axis, indicating single ionization, but differ in their distribution off the axes, representing double ionization. While Hartree–Fock fails completely to account for double ionization, higher configuration calculations do exhibit two-electron detachment. None of the tested configurations shows the pronounced avoidance of the wavefunction along the potential ridge ($x = y$), which is a known artifact of TDHF methods [11, 16]. MCTDHF still does not correctly reproduce two-electron distributions, but total double ionization is well reproduced, as will be demonstrated below.

We now turn to a more quantitative investigation of the ionization process. To this end we define various multi-photon absorption probabilities [16, 27] and calculate them at the end of the laser pulse at time $t = 6T_L$, where $T_L = 2\pi/\omega$ denotes the cycle duration of the laser. The probability of being in the ground state is estimated by

$$P^0 = |\langle \Psi(x, y; 0) | \Psi(x, y; 6T_L) \rangle|^2. \tag{20}$$

For an estimate of total bound state population after the pulse we replace the (unknown) excited two-electron bound states of the system by products of single-electron bound states. Let ϕ_i denote a complete set of field-free bound states for the atomic ion. The probability of finding two electrons in bound states is then estimated as

$$\sum_{i,j} P_{i,j} = \sum_{i,j} |\langle \phi_i(x)\phi_j(y) | \Psi(x, y; 6T_L) \rangle|^2. \tag{21}$$

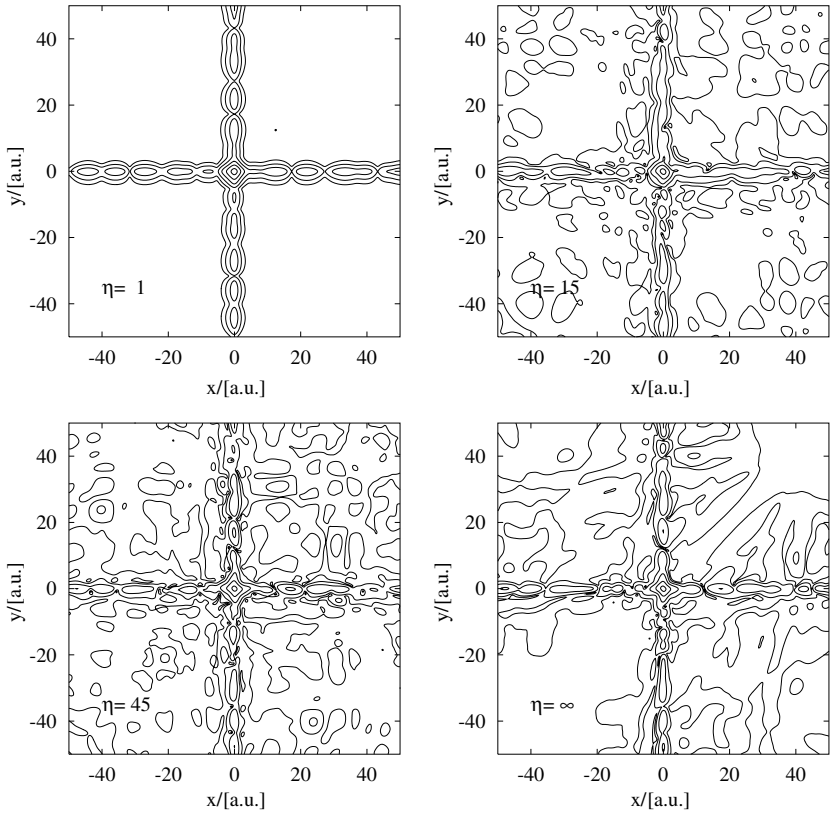

Figure 4. Logarithmic contour maps of the probability density of helium at the end of the laser pulse (peak intensity $I = 1.26 \times 10^{15}$ W cm^{-2}) for various configurations η. ($\eta = \infty$ refers to the numerically exact solution.) Contours differ by a factor of 10.

The probability P^+ of single ionization is calculated as

$$P^+ = 2 \sum_i \left[\int \mathrm{d}x |\langle \phi_i(y) | \Psi(x, y; 6T_L) \rangle|^2 - \sum_j P_{i,j} \right] \tag{22}$$

while the double ionization probability P^{2+} is given by

$$P^{2+} = 1 - P^+ - \sum_{i,j} P_{i,j}. \tag{23}$$

Finally we get the total ionization probability

$$P^{\mathrm{tot}} = P^+ + P^{2+}. \tag{24}$$

Table 3 lists the total ionization probabilities depending on the number of MCTDHF configurations η for two different intensities. We first note that at both intensities ionization is underestimated. Further, table 3 confirms the insufficiency of TDHF. Including more configurations does significantly reduce the error, resulting in errors of roughly 5% for $\eta \geqq 28$. A further reduction of the error is possible, but with soaring costs.

At an intensity of $I = 1.26 \times 10^{15}$ W cm^{-2} significant double ionization takes place as can be seen in table 4, where the multi-photon ionization probabilities are listed. As figure 4

Table 3. Probability of total ionization P^{tot} of a 1D helium atom at different intensities for an increasing number of configurations η. $\eta = \infty$ refers to the numerically exact values.

		$I = 1.26 \times 10^{15}$ W cm^{-2}		$I = 5.00 \times 10^{15}$ W cm^{-2}	
n	$\eta = \binom{n}{2}$	P_η^{tot}	$\frac{P_\eta^{\text{tot}} - P_\infty^{\text{tot}}}{P_\infty^{\text{tot}}}$	P_η^{tot}	$\frac{P_\eta^{\text{tot}} - P_\infty^{\text{tot}}}{P_\infty^{\text{tot}}}$
2	1	0.1548	−0.4120	0.7936	−0.0978
4	6	0.2210	−0.1606	0.8474	−0.0367
6	15	0.2241	−0.1488	0.8265	−0.0604
8	28	0.2476	−0.0596	0.8323	−0.0538
10	45	0.2485	−0.0565	0.8325	−0.0536
12	66	0.2555	−0.0296	0.8388	−0.0464
∞	∞	0.2633	0.0000	0.8797	0.0000

Table 4. Multi-photon ionization of a 1D helium atom at an intensity of $I = 1.26 \times 10^{15}$ W cm^{-2} for an increasing number of configurations η. $\eta = \infty$ refers to the numerically exact values.

n	$\eta = \binom{n}{2}$	P_η^0	$\frac{P_\eta^0 - P_\infty^0}{P_\infty^0}$	P_η^+	$\frac{P_\eta^+ - P_\infty^+}{P_\infty^+}$	P_η^{2+}	$\frac{P_\eta^{2+} - P_\infty^{2+}}{P_\infty^{2+}}$
2	1	0.8923	0.1032	0.1488	−0.3734	0.0059	−0.7859
4	6	0.8533	0.0550	0.1963	−0.1734	0.0246	−0.0428
6	15	0.8308	0.0272	0.2051	−0.1364	0.0189	−0.2645
8	28	0.8264	0.0217	0.2225	−0.0631	0.0250	−0.0272
10	45	0.8188	0.0123	0.2201	−0.0732	0.0283	0.1011
12	66	0.8129	0.0050	0.2281	−0.0395	0.0273	0.0622
∞	∞	0.8088	0.0000	0.2375	0.0000	0.0257	0.0000

implies, the TDHF approximation fails completely to describe double ionization, but higher configurations do agree on predicting double ionization probabilities of about 2.5%. Even with six configurations one can already account for the essential physics, predicting a four-times-higher double ionization probability than TDHF. Convergence to results better than that needs a large number of configurations, making the calculation computationally expensive.

5. Conclusions

We have demonstrated that by systematic inclusion of correlation the MCTDHF method provides a good approximation of time-dependent multi-electron wavefunctions. We have tested our approach on two highly correlated two electron systems. For bound state dynamics MCTDHF provides a rapidly convergent expansion. For ionizing systems MCTDHF is capable of describing the strongly correlated process of double ionization correctly. A quantitative description of single and double ionization within an accuracy of 5% can be achieved with a reasonable number of configurations. We have detected no artifacts of the method as they were reported about time-dependent density functional theory [28]. From a computational point of view, the key property of the method is the favourable scaling behaviour when compared to straightforward discretization of a multi-electron system. Whereas the number of points in straightforward discretization increases exponentially with the number of particles f, MCTDHF scales linearly $\propto n \geqslant f$ for the factor functions φ. The demonstrated convergence behaviour and moderate increase of problem size with the number of electrons make MCTDHF a powerful approach for the calculation of the correlated dynamics of many-electron systems

in strong fields, where calculations with up to ten active electrons and a significant amount of correlation may be feasible.

The present demonstration of the MCTDHF method is only in 1D. The main challenge for extending the method to 3D is finding a discretization of the 3D factor functions $\varphi(\vec{x})$, which allows efficient computation of 3D and 6D integrals. In [19] a reduction of high-dimensional integrals (here 6D) to lower dimensions (3D) by a product representation is described, which naturally matches the product expansion of the solution. For the 3D discretization itself, a variety of strategies are being investigated, including discrete variable representations, self-adaptive grids, and 'cascading' or 'multilayer' techniques as described in [29, 30]. It is important to note that the extension to 3D, in principle, only affects the factor functions, whereas the scaling behaviour with respect to f and n is independent of dimensionality. In practice, correlations in 3D may be more pronounced, requiring longer expansions and adding additional complexity to an MCTDHF calculation.

Acknowledgment

This work was supported by the Austrian Science Fund special research program F011 and project Y142-TPH.

References

[1] Ammosov M V, Delone N B and Krainov V P 1986 *Sov. Phys.–JETP* **64** 1191
[2] Kulander K C 1987 *Phys. Rev.* A **35** 445
[3] Schafer K J *et al* 1993 *Phys. Rev. Lett.* **70** 1599
[4] Lezius M *et al* 2001 *Phys. Rev. Lett.* **86** 51
[5] Lezius M *et al* 2002 *J. Chem. Phys.* **117** 1575
[6] Zhang J and Lambropoulos P 1995 *J. Phys. B: At. Mol. Opt. Phys.* **28** L101
[7] Burke P G and Burke V M 1997 *J. Phys. B: At. Mol. Opt. Phys.* **30** L383
[8] Parker J *et al* 2000 *J. Phys. B: At. Mol. Opt. Phys.* **33** L691
[9] Runge E and Gross E K U 1984 *Phys. Rev. Lett.* **52** 997
[10] Bauer D 1997 *Phys. Rev.* A **56** 3028
[11] Kulander K C 1987 *Phys. Rev.* A **36** 2726
[12] Kulander K C 1988 *Phys. Rev.* A **38** 778
[13] Pindzola M S, Griffin D C and Bottcher C 1991 *Phys. Rev. Lett.* **66** 2305
[14] Pindzola M S, Gorczyca T W and Bottcher C 1993 *Phys. Rev.* A **47** 4982
[15] Pindzola M S, Gavras P and Gorczyca T W 1995 *Phys. Rev.* A **51** 3999
[16] Pindzola M S, Robicheaux F and Gavras P 1997 *Phys. Rev.* A **55** 1307
[17] Froese Fischer C, Brage T and Jonsson P 1997 *Computational Atomic Structure: An MCHF Approach* (Bristol: Institute of Physics Publishing)
[18] Zanghellini J *et al* 2003 *Laser Phys.* **13** 1064
[19] Beck M H *et al* 2000 *Phys. Rep.* **324** 1
[20] Dirac P A M 1930 *Proc. Cam. Phil. Soc.* **26** 376
[21] Frenkel J 1934 *Wave Mechanics* (Oxford: Clarendon)
[22] Kulander K C, Shafer K J and Krause J L 1992 *Atoms in Intense Laser Fields* (London: Academic) p 247
[23] Mercouris Th *et al* 1994 *Phys. Rev.* A **50** 4109
[24] Su Q and Eberly J H 1991 *Phys. Rev.* A **44** 5997
[25] Schwengelbeck U 1999 *Phys. Lett.* A **253** 168
[26] Grobe R, Rzazewski K and Eberly J H 1994 *J. Phys. B: At. Mol. Opt. Phys.* **27** L503
[27] Grobe R and Eberly J H 1994 *Phys. Rev.* A **48** 4664
[28] Veniard V, Taieb R and Maquet A 2003 *Laser Phys.* **13** 465
[29] Meyer H-D and Worth G A 2003 *Theor. Chem. Acc.* **109** 251
[30] Wang H and Thoss M 2003 *J. Chem. Phys.* **119** 1289